

Failure Criterion of an Asphalt Mixture under Three-dimensional Stress State

T. Huang¹, J.L. Zheng¹, S.T. Lv¹, J.H. Zhang^{1*}, P.H. Wen², C.G. Bailey²

¹National Engineering Laboratory of Highway Maintenance Technology, Changsha University of Science & Technology, Changsha, 410114, China.

²School of Engineering and Materials Science, Queen Mary University of London, London E1 4NS, UK.

*Correspondence: zjhseu@csust.edu.cn.

Abstract: A self-developed triaxial test method was adopted to characterize mechanical behavior of the asphalt mixture under three-dimensional stress states in this study. The conventional uniaxial tests and triaxial tests were conducted in the laboratory to verify the triaxial test results obtained using the technique developed. It is shown that the three-dimensional stress states affect significantly the ultimate failure strength of AC-13 asphalt mixture and the failure modes are mainly represented both for the tensile failure and shear failure. The nonlinear strength criterion, as well as a linear engineering model of asphalt mixture under three-dimensional stress states in $\sigma_{oct} - \tau_{oct}$ space, was established based on the triaxial compressive/tensile tests, the plane tensile and compressive/axial tensile tests. In addition, a new method to carry out the strength design of asphalt pavement under the three-dimensional stress state was given to consider the failure effect of each stress component to the asphalt pavements.

Key words: Asphalt mixture; triaxial test; three-dimensional stress state; failure criterion; simplified strength model

1. Introduction

At present, 136 thousands kilometers expressway has been built in China, in which more than 90% uses the asphalt pavement structure. In addition, 40~50 thousands kilometers expressway with the asphalt pavement will be constructed by 2030. The design method of the asphalt pavement in China belongs to the mechanical-empirical method and the elastic layered half-space is modeled to calculate the mechanical responses of pavements. The theories of strength with the maximum tensile stress and maximum tensile strain are used as the failure criteria for asphalt pavements.

In general, the pavement works under complex stress states subjected to the traffic loading and thermal effects [1,2,3]. The ordinary strength test such as the uniaxial tensile test [4,5], uniaxial compression test [6,7], bending test [8,9,10] and indirect tensile test [11,12] under simple

1 stress states cannot be applied to simulate the real multi-axial stress conditions in the pavement
2 structures. Apparently the tensile strength of asphalt materials under one-dimensional or
3 two-dimensional stress state can not represent the failure characteristics of asphalt pavements. Due
4 to the conventional triaxial test is available only for the triaxial compressive tests with a low
5 confining pressure [13,14,15,16,17], it is difficult to study the failure criterion of asphalt mixtures
6 using this test.

7 Due to the limits of the test equipment, few researchers carried out the study on the failure
8 criterion of asphalt mixtures under complex stress states. Wang et al.[18] proposed a nonlinear
9 failure envelop in $I_1 - \sqrt{J_2}$ space based on the failure strength results of the dense asphalt
10 concrete. Desai et al.[19] proposed a response surface for asphalt materials and utilized it as the
11 response function of the yield surface. It can be applied both in the stress invariant and strain
12 variant space. Nevertheless, three-dimensional unequal stress state was not established and the
13 failure criterion was not verified by true triaxial results in a three-dimensional stress state, especially
14 at a triaxial tensile stress state. Guan et al. [20] carried out three-directional compression strength
15 tests for three kinds of asphalt mixtures at -10°C with a self-developed simplified triaxial machine,
16 the tested data of strength on the π -plane are close to a twin shear theory contour curve without
17 the triaxial tensile strength consideration. In general, the tensile performance rather than the shear
18 performance should be considered for asphalt mixtures in a low temperature [21]. Therefore, it is
19 necessary to make efforts to establish the strength criterion of asphalt
20 mixtures under three-dimensional stress states, in which the effects of triaxial tensile strength should
21 be considered. So, the main objective of this paper is to establish the failure criterions under
22 three-dimensional stress states. Moreover, a new design method to carry out the strength design of
23 asphalt pavements was presented under three-dimensional stress states.

24

25 **2. Test methods and specimen preparation**

26 *2.1. Materials and specimens*

27 In order to evaluate the mechanical behavior of asphalt mixtures under three dimensional
28 stress states, the representative AC-13C asphalt mixture which were widely used in China were
29 tested. As shown in Fig.1, the aggregate particles of AC-13C asphalt mixture are continuously
30 graded to form an interlock structure. The performances of mixtures tested extensively can be
31 referred from the results of Huang [22], in which the SBS modified bitumen was used as the binder
32 and the basalt was used as aggregates.

33

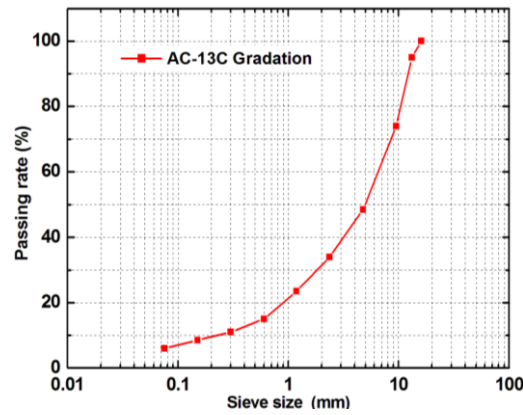


Fig1. Gradation curve of AC-13C asphalt mixture.

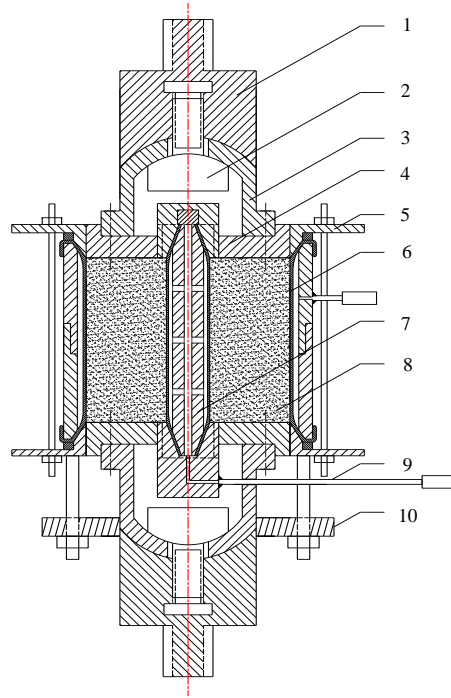
1
2
3
4
5
6
7
8
9

To ensure the consistency of specimen in the triaxial test, the gyratory compactor was used to prepare cylindrical specimens with 102mm in height and 100mm in diameter. The bitumen-aggregates weight ratio of 5.2% was selected with the air void content for these specimens of $4.5\% \pm 0.5\%$. Moreover, the tested specimens were obtained by sawing the two ends of original specimens in the water with a diamond blade up to the height of 100mm.

2.2. Test equipment and method

10
11
12
13
14
15
16

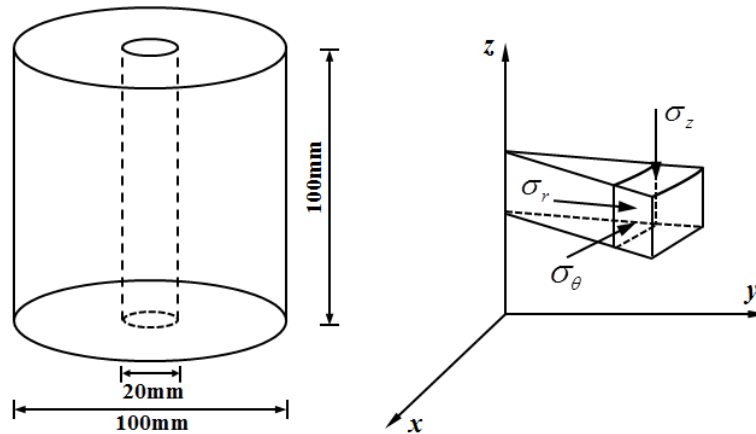
The triaxial test system developed by Zheng and Huang is shown in Fig.2[22,23]. For this testing system, a hollow cylinder specimen with an inner radius r_a and outer radius r_b was placed in the triaxial test equipment while the inner and outer surfaces of specimens were loaded by two flexible airbags respectively. Using these airbags, the adjustable radial compressive stress and circumferential tensile stress can be produced consequently. A sketch of hollow cylinder specimen with dimensions and element with principle stresses are shown in Fig.3.



1
2
3
4
5
6

Fig. 2 Loading structure schematic diagram of triaxial testing equipment.

Note: 1-loading rod, 2-ball hinge pin, 3-hemispherical head compressive(tensile)tip,
4-compressive(tensile) plate, 5-outer airbag cover, 6-outer airbag, 7-inner airbag, 8-specimen, 9-trachea,
10-outer airbag tray



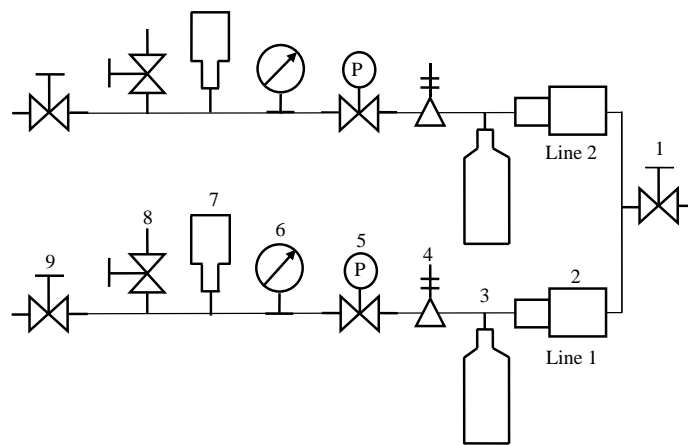
7
8
9

Fig. 3 A sketch of hollow cylinder specimen and the principle stresses with elements.

10 The output from 0MPa to 6MPa with the control precision of 0.01MPa can be obtained by
11 those two airbags connected to the pressure control system, as shown in Fig.4. When the main
12 switch is open, the air is compressed into the high pressure vessel by the booster pump with a
13 compression proportion of 6:1. In such control system, two passages are designed in order to isolate

1 the pressures from inner and outer airbags. However, it is observed that the booster pump works in
 2 an intermittent condition and the export pressure of booster pumps are unstable. Whereas, the
 3 pulsation of pressure is significantly attenuated after the air enters the high pressure vessel and goes
 4 through the high pressure valve while the pressure value is reduced. Thereafter, the stable and
 5 reliable gas pressures can be obtained. The pressure reduced is measured with a high precision
 6 pressure gauge, pressure sensor, pressure relief valve and output valve. The function of
 7 measurement with the pressure sensor is to obtain the pressure using the electrical signals output
 8 with a computer. The outputs of pressure are also used to adjust the pressures in those two
 9 airbags. And the gas pressure is obtained with the high precision pressure gauges.

10



11
 12 Fig.4 Schematic diagram of pressure control system

13 Note: line 1-gas passage of inner airbag, line 2-gas passage of outer airbag, 1-main switch,
 14 2-booster pump, 3-high pressure vessel, 4-high pressure valve, 5-pressure reducing
 15 valve, 6-precision pressure gauge, 7-pressure sensor, 8-pressure relief valve, 9-output valve

16

17 The upper and lower surfaces of specimen are loaded through a rigid loading shaft of MTS
 18 material testing machine with axial tensile or compressive forces. When the axial force is less than
 19 100kN, it is provided by the MTS landmark test system with the maximum load of 100KN. Then
 20 the triaxial tests of specimens are conducted on no less than three effective duplicates. However,
 21 when the axial force is close/more than 100kN, it is provided by the MTS civil structure test
 22 system with the maximum load of 750KN. Different from the frame structure of MTS landmark
 23 test system, the MTS civil structure test system is a suspended structure. Therefore, the axial
 24 loading should be guaranteed during the test process. Otherwise, the airbags with their
 25 components might be damaged. So, the triaxial tests of specimens are conducted on no less than
 26 two effective duplicates when MTS civil structure test system is adopted. It is obvious that the
 27 working condition in a three-dimensional unequal stress state can be generated to simulate the

1 complex stress state in asphalt concrete materials in the pavement structures. The axial stress, σ_z ,
 2 radial stress, σ_r , and circumferential stress, σ_θ , are determined as follows:

$$3 \quad \sigma_z = \frac{P}{\pi(r_b^2 - r_a^2)} \quad (1)$$

$$4 \quad \sigma_r = -\frac{r_b^2 / r^2 - 1}{r_b^2 / r_a^2 - 1} P_a - \frac{1 - r_a^2 / r^2}{1 - r_a^2 / r_b^2} P_b \quad (2)$$

$$5 \quad \sigma_\theta = \frac{r_b^2 / r^2 + 1}{r_b^2 / r_a^2 - 1} P_a - \frac{1 + r_a^2 / r^2}{1 - r_a^2 / r_b^2} P_b \quad (3)$$

6 where P in Eq. (1) is the axial failure load; r is the distance between observing point in the
 7 specimen to the symmetric center of the hollow cylindrical specimen; P_a and P_b are the inner
 8 and outer pressures; r_a and r_b are the inner and outer radius of the hollow cylinder specimen,
 9 respectively. According to the elastic mechanics, σ_r , σ_θ and σ_z are the principal stresses,
 10 which can be sorted by numerical values (tensile stress is positive and compressive stress is
 11 negative) with principal stresses σ_1 , σ_2 and σ_3 , respectively.

12

13 2.3. Description of the failure criterion under three dimensional stress state

14 As shown in Fig.5, in the principal stress space, the isoclinic line (line n) has the same
 15 direction angle with the principal stress axes $\sigma_1, \sigma_2, \sigma_3$, and perpendicular to the isoclinic
 16 plane. The projection of principal axes on the isoclinic plane are generally represented by axes σ_1' ,
 17 σ_2' , σ_3' , and the intersection angles among two of them are 120° . The projection of any point P in
 18 the isoclinic line is the octahedral normal stress σ_{oct} . Its projection in the isoclinic plane is the
 19 octahedral shear stress τ_{oct} . The direction is represented by lode angle θ [24,25]. All of these
 20 parameters are defined as follows:

$$21 \quad \sigma_{oct} = (\sigma_1 + \sigma_2 + \sigma_3) / 3 = \sigma_m \quad (4)$$

$$22 \quad \tau_{oct} = \sqrt{(\sigma_1 - \sigma_2)^2 + (\sigma_2 - \sigma_3)^2 + (\sigma_3 - \sigma_1)^2} / 3 \quad (5)$$

$$23 \quad \theta = \arccos \left[(2\sigma_1 - \sigma_2 - \sigma_3) / (3\sqrt{2}\tau_{oct}) \right] \quad (6)$$

24

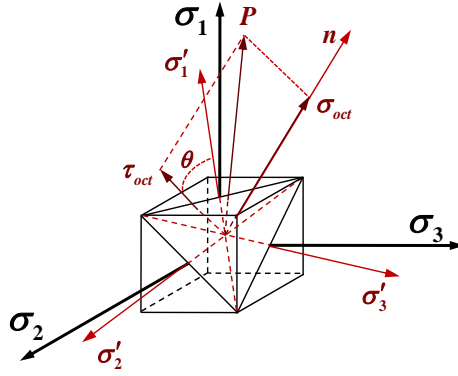


Fig.5 Octahedral normal stress, octahedral shear stress and lode angle

All points for material failure can constitute a continuous surface which is called the failure envelope surface, as shown in Fig.6. The intersection curve of failure envelope surface and isoclinic plane is called the failure envelope curve. Failure envelope curves are closed. Their sizes change with the change of the average stress σ_m ($\sigma_m = \sigma_{oct}$) and their shapes are similar.

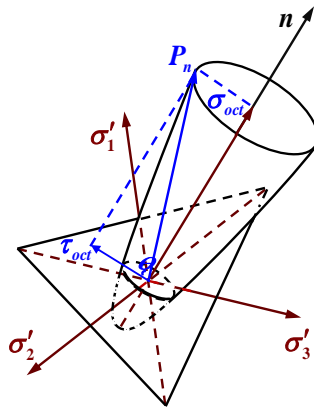
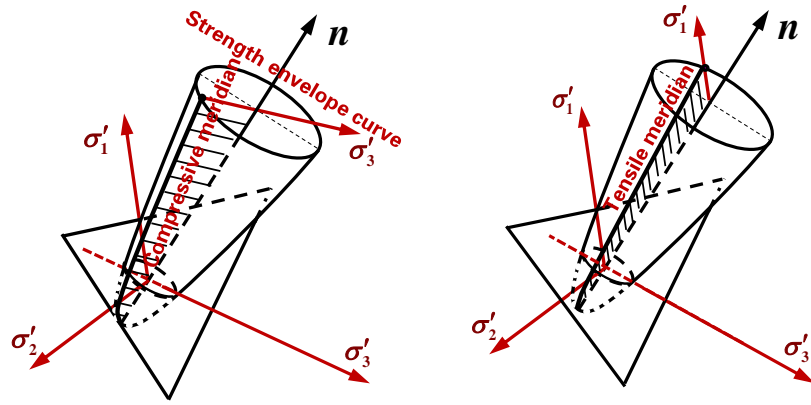


Fig.6 Failure envelope surface

For an isotropic material, the axes $\sigma'_1, \sigma'_2, \sigma'_3$ on the isoclinic plane are the symmetric axes of the failure envelope curve. If the strength envelope curve from $0^\circ \sim 60^\circ$ can be obtained, the whole strength envelope can be achieved. To obtain the failure envelope curve, the strength test should be done at the same σ_m , and the lode angle should be changed from $0^\circ \sim 60^\circ$ gradually.

As shown in Fig. 7(a), the compressive meridian is a curve on the failure envelope surface which is formed by all the points with a 60° lode angle, and can be obtained by the strength test under different average stresses σ_m , as well as lode angle $\theta = 60^\circ$. Likewise, the tensile meridian can be gained when the lode angle is 0° , as shown in Fig.7(b).



(a)Compressivemeridian and failure envelope curve; (b)Tensile meridian

Fig.7Compressive,tensile meridian and failure envelope curves

2.4. Testing conditions and procedures

2.4.1 Testing conditions

For a triaxial test, 15°C was chosen as the testing temperature and the axial loading rate was 2mm/min. The testing conditions are the same as the uniaxial compressive test in the current specification of *Standard Test Methods of Bitumen and Bituminous mixtures for Highway Engineering* (JTG E20-2011) in China. Moreover, the dimensions of the hollow cylinder specimens were selected by coring solid cylinder specimens with a dimension of 10mm×50mm×100mm (inner radius × out radius × length). The length and diameter of specimens are also the same as the standard uniaxial compressive test in China. So, it is easy to verify the accuracy of test results. The specimens with the two ends polished were placed into a temperature control chamber for more than 6 hours. The lubricant oil was smeared on the specimen surfaces and loading plates to reduce the friction for the triaxial compressive test. The epoxy resin was smeared on the specimen surfaces and loading plates to firmly bond for the triaxial tensile test.

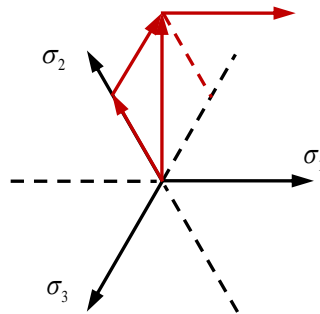
2.4.2 Test procedures

In the octahedral stress space, the failure envelope curve, tensile meridian and compressive meridian can be used to describe the strength criterion under three dimensional stress states as mentioned above [24]. The test procedures are as follows [22,23]:

(1) Determine the failure envelope curve. The plane tensile and compressive/axial tensile tests were fulfilled with a constant average stress and the lode angles from 0°~60° changed gradually. For this test, the transverse stress, that is σ_2 and σ_3 , increased up to the pre-determined values proportionally first by applying pressure by the inner air bag, and thereafter the axial tensile

1 stress, σ_1 , was inputted by MTS material testing machine until the failure of specimen. The stress
 2 path of failure envelope curve is shown in Fig.8.

3



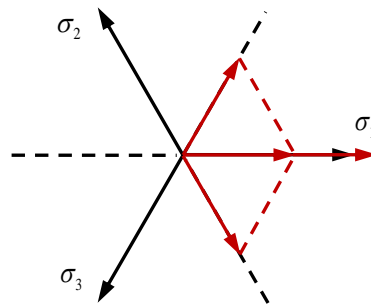
4

5 Fig.8 Stress path of failure envelope curve.

6

7 (2) Determine the tensile meridian. The tensile meridian can be obtained by the triaxial tensile
 8 test, that is a strength test with different average stresses, σ_m , while the lode angle θ was equal to
 9 0° . In this test, the transverse stresses σ_2 and σ_3 ($\sigma_2 = \sigma_3$) increase to the pre-determined values
 10 first by applying synchronously equal pressures with inner and outer airbags, and thereafter the
 11 axial tensile stress, σ_1 , was applied by using MTS until the specimen breaks. The stress path of
 12 tensile meridian is shown in Fig. 9.

13



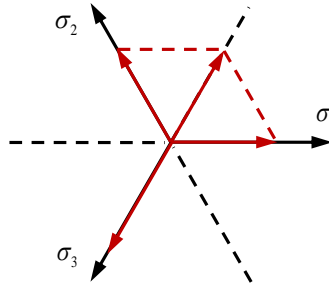
14

15 Fig.9 Stress path of tensile meridian.

16

17 (3) Determine the compressive meridian. The compressive meridian can be obtained by the
 18 triaxial compressive test, i.e. the strength test under different average stresses, σ_m , when the lode
 19 angle θ was equal to 60° . For this test, the transverse stresses σ_1 and σ_2 ($\sigma_1 = \sigma_2$) were applied
 20 to the pre-determined values first by applying synchronously equal pressures with inner and outer
 21 airbags, and then the axial compressive stress σ_3 was exerted by MTS until the specimen breaks. The
 22 stress path of compressive meridian is shown in Fig.10.

1



2

3

Fig.10 Stress path of compressive meridian.

4

5 3. Failure criteria

6 3.1. Nonlinear failure criterion under complex stress state

7 The results of triaxial compressive/tensile tests, the plane tensile and compressive/axial
8 tensile tests are presented in Appendix for reference [22,23]. Based on the test results, the
9 failure criteria of asphalt mixtures under three-dimensional stress states are given as follows:

10 Tensile meridian:

$$11 \quad \tau_{oct}^t / \sigma_c = 0.085 - 0.57 \sigma_{oct} / \sigma_c - 0.588 (\sigma_{oct} / \sigma_c)^2 \quad R^2 = 0.96 \quad (7)$$

12 Compressive meridian:

$$13 \quad \tau_{oct}^c / \sigma_c = 0.13 - 0.967 \sigma_{oct} / \sigma_c - 0.17 (\sigma_{oct} / \sigma_c)^2 \quad R^2 = 0.98 \quad (8)$$

14 Failure envelope curve:

$$15 \quad \tau_{oct}(\theta) = \tau_{oct}^t - (\tau_{oct}^t - \tau_{oct}^c) \sin^6(3\theta / 2) \quad R^2 = 0.94 \quad (9)$$

16 where σ_c is the uniaxial compressive strength; σ_{oct} is the octahedral normal stress, τ_{oct} is the
17 octahedral shear stress; θ is the lode angle; τ_{oct}^t is the octahedral shear stress in the tensile
18 meridian; τ_{oct}^c is the octahedral shear stress in the compressive meridian.

19 These failure criteria can be verified with the uniaxial tensile strength test, uniaxial
20 compressive strength test as well as the conventional triaxial test [22]. Moreover, the criteria are
21 suitable for calculating the resistances under various stress states.

22 For the triaxial tensile test, the plane tensile and compressive/axial tensile test specimens
23 failures are shown in Fig. 11. For triaxial compressive test, the specimens are broken mainly due
24 to the shear failure shown in Fig. 12 [22,23].

25



Fig.11 Tensile failure. Fig.12 Shear failure.

Since there are many free parameters in this failure criterion, the equation of criterion becomes complicated. In addition, the confining pressures in the pavement structure are relatively small and usually less than 1MPa. In order to simulate the real multi-axial stress conditions in the pavement structures, the tensile meridian could be approximated with a quadratic polynomial, and the tensile and compressive meridians must intersect at the same point when $\tau_{oct}=0$ [24]. It is assumed that the strength envelope in the region of $0^\circ \sim 60^\circ$ is interpolated with the sine function. Therefore, the tensile meridian, compressive meridian and failure envelope curves can be represented, in Fig.13,14 [22,23], as

Tensile meridian:

$$\tau_{oct}^t / \sigma_c = a - b\sigma_{oct} / \sigma_c - c(\sigma_{oct} / \sigma_c)^2 \quad R^2 = 0.95 \quad (10)$$

Compressive meridian:

$$\tau_{oct}^c / \sigma_c = m \left[a - b\sigma_{oct} / \sigma_c - c(\sigma_{oct} / \sigma_c)^2 \right] \quad R^2 = 0.97 \quad (11)$$

Failure envelope curve:

$$\tau_{oct}(\theta) = \tau_{oct}^t - (\tau_{oct}^t - \tau_{oct}^c) \sin^n(3\theta/2) \quad R^2 = 0.95 \quad (12)$$

where a, b, c, m and n are model parameters as shown in Table 1.

Table 1 Model parameters of the nonlinear failure criterion

Model parameters	a	b	c	m	n
Fitting results	0.085	0.56	0.01	1.49	7

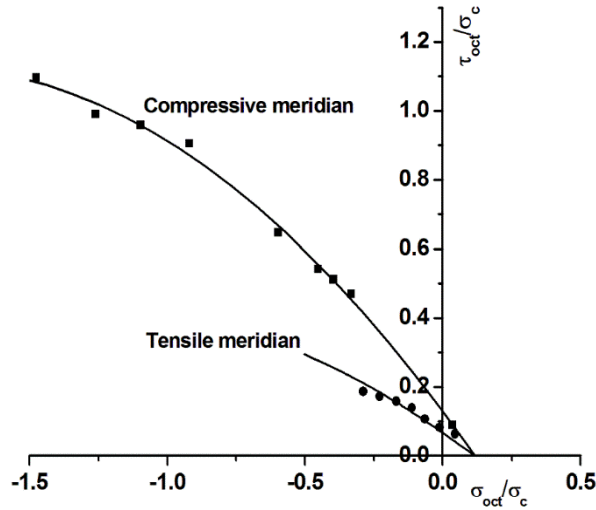


Fig.13 Nonlinear compressive meridian and tensile meridian.

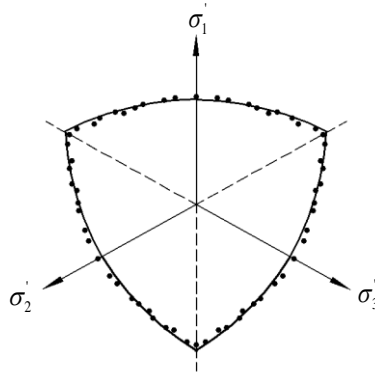


Fig.14 Nonlinear failure envelope curve in π - plane ($\sigma_m=0.286\text{MPa}$).

3.2. Simplified linear failure criterion under complex stress state

In engineering analysis, it is difficult to establish nonlinear strength criteria of asphalt mixtures for a pavement structure design. Because different mixtures have different failure envelope surfaces and engineering design department does not possess all testing conditions to establish the failure envelope surface, the nonlinear failure envelope surface should be simplified for the sake of analysis convenience in engineering design.

Usually, the normal stress σ_{oct} is less than one-third of the uniaxial compressive strength σ_c in pavement structures. Therefore, the test results can be fitted linearly in general stress range. The failure criterion established by linear fitting is found to be safer than the nonlinear fitting. Therefore, the criterion of strength could be simplified as a linear envelope which is called as engineering model of strength criterion. Assuming that the engineering model is linear as below

Tensile meridian:

1
$$\tau_{oct}^t / \sigma_c = A - B\sigma_{oct} / \sigma_c \quad R^2 = 0.95 \quad (13)$$

2 Compressive meridian:

3
$$\tau_{oct}^c / \sigma_c = M[A - B\sigma_{oct} / \sigma_c] \quad R^2 = 0.96 \quad (14)$$

4 Failure envelope curve:

5
$$\tau_{oct}(\theta) = \tau_{oct}^t - (\tau_{oct}^t - \tau_{oct}^c)3\theta / \pi \quad R^2 = 0.83 \quad (15)$$

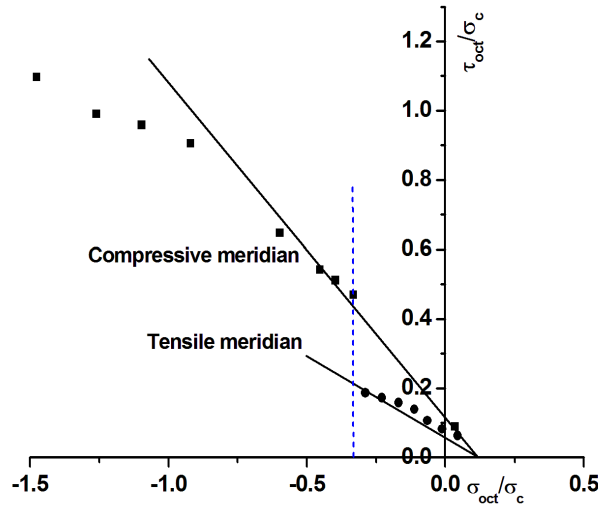
6 where A, B and M are model parameters as shown in Table 2.

7

8 Table 2. Model parameters of the linear engineering model

Model parameters	A	B	M
Fitting results	0.074	0.59	1.65

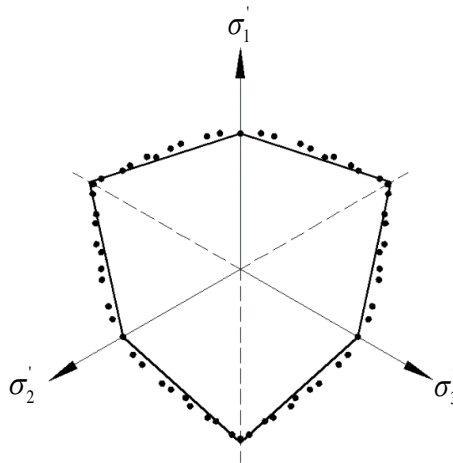
9



10

11

Fig.15 Linear compressive meridian and tensile meridian.



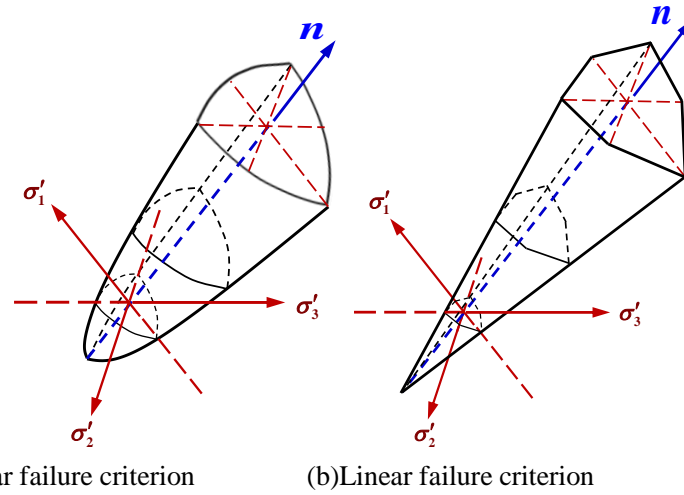
12

13

Fig.16 Linear Failure envelope curve in π - plane ($\sigma_m = 0.286$ MPa)

1 The comparison between the nonlinear strength model of quadratic polynomial and the linear
 2 engineering model of asphalt mixtures in $\sigma_{oct} - \tau_{oct}$ space is shown in Fig. 17.

3



4

5

6

7

8

9

10

11

12

13

14

15

16

17

18

19

20

21

22

23

24

25

26

27

Fig.17 Comparison of failure criteria in the $\sigma_{oct} - \tau_{oct}$ space.

Seeing from Fig. 16 and Fig. 17, it is clear that the nonlinear failure envelope of asphalt mixtures transformed from the cone which is similar to a shield into a pyramid in the $\sigma_{oct} - \tau_{oct}$ space due to the linear regression. Therefore, it is more convenient for asphalt pavement design.

By using the same technique, a simplified strength model under three-dimensional stress states can be established by triaxial compressive and triaxial tensile tests. It is not difficult to establish the failure envelope surface for the design of pavement structures with the consideration of the effect of each stress component to the failure analysis in asphalt pavements. Furthermore, the strength analysis process of the asphalt pavements under three-dimensional stress states can be carried out with the following steps:

(1) The determination of fatigue strength reduction coefficient K of each structure layer based on fatigue tests. The simplification of the strength criteria of each structural layer under three-dimensional stress states based on triaxial compressive/tensile tests;

(2) The stress state analysis at any points of pavement under vehicle/thermal loads by layered elastic half space modeling;

(3) The determination of octahedral normal stress σ_{oct} , shear stress τ_{oct} and load angle θ at any point of pavement;

(4) The evaluation of stress components to the AC-13 layer of pavement structure by

$$\tau_{oct}(\theta) \leq \left[\tau_{oct}^t - (\tau_{oct}^t - \tau_{oct}^c) 3\theta / \pi \right] / K \quad (16)$$

Where K can be taken as 1;

(5) Carry out the strength design of other structural layers of asphalt pavement according to the

1 above steps. So, the strength design of asphalt pavement can be completed.
2

3 **4. Conclusions and discussion**

4 The nonlinear failure criteria were proposed based on the test results of AC-13C asphalt
5 mixture under three dimensional stress states. It was observed that the failure strength and failure
6 mode of AC-13C asphalt mixtures were affected significantly by the stress states. The nonlinear
7 failure criteria of asphalt mixtures under three-dimensional stress states were validated with
8 triaxial compressive/tensile tests and plane tensile/compressive/axial tensile tests. The difference
9 between the tensile and compressive strength was shown clearly. The criteria proposed in this
10 study are suitable to determine the resistance under various stress state.

11 The simplified linear failure criteria for engineering design were also proposed based on the
12 triaxial compressive/tensile tests. These criteria are in a simple form and easy to use in asphalt
13 pavement structural design. Moreover, this technique can be extended semi-rigid base. Based on
14 these investigations, a new method to carry out the strength design of asphalt pavement under the
15 three-dimensional stress state is presented with the consideration of the effect of each stress
16 components to the failure analysis in asphalt pavements.

17 Although this study has many advantages, the triaxial test should be fulfilled for different
18 asphalt concrete materials in order to establish more reliable three-dimensional failure criteria.
19 The further study on the strength design method under three-dimensional stress state should be
20 carried out before it is applied to engineering practice.
21

22 **Acknowledgments**

23 This work was supported by the National Natural Science Foundation of China (No: 51608055,
24 51478054) and partially supported by Natural Science Foundation of Hunan Province (No:
25 2017JJ3337); Science Research Project of Hunan Provincial Education Department under (No:
26 16C0051); Open Fund of the Key Laboratory of Highway Engineering of Ministry of Education
27 (Changsha University of Science & Technology) (No: kfj160201); Planned Science and Technology
28 Project of Changsha city 2017 (No: kq1701078); Construction Project of Science and Technology
29 of Ministry of Transport of the People's Republic of China (No: 2015318825120).
30

31 **Appendix**

32 A: Results of triaxial compressive tests

σ_1 /MPa	σ_2 /MPa	σ_3 /MPa	Average value	$\frac{\sigma_{oct}}{\sigma_c}$	$\frac{\tau_{oct}}{\sigma_c}$	$\theta / ^\circ$
-----------------	-----------------	-----------------	------------------	---------------------------------	-------------------------------	-------------------

0	0	-6.986		-0.326	0.462	60
0	0	-7.263	-7.135	-0.339	0.480	60
0	0	-7.156		-0.334	0.473	60
-0.250	-0.250	-7.910		-0.393	0.506	60
-0.250	-0.250	-8.250	-7.989	-0.409	0.529	60
-0.250	-0.250	-7.806		-0.388	0.499	60
-0.500	-0.500	-8.766		-0.456	0.546	60
-0.500	-0.500	-8.810	-8.679	-0.458	0.549	60
-0.500	-0.500	-8.460		-0.442	0.526	60
-1.000	-1.000	-10.265		-0.573	0.612	60
-1.000	-1.000	-11.089	-10.776	-0.611	0.667	60
-1.000	-1.000	-10.973		-0.606	0.659	60
-2.000	-2.000	-16.239		-0.946	0.941	60
-2.000	-2.000	-15.064	-15.652	-0.891	0.863	60
-3.000	-3.000	-17.124		-1.080	0.933	60
-3.000	-3.000	-17.777	-17.451	-1.111	0.976	60
-4.000	-4.000	-18.636		-1.244	0.967	60
-4.000	-4.000	-19.400	-19.018	-1.280	1.017	60
-5.000	-5.000	-21.134		-1.455	1.066	60
-5.000	-5.000	-22.014	-21.574	-1.496	1.124	60

1

2

B: Results of triaxialtensile tests

σ_1 /MPa	σ_2 /MPa	σ_3 /MPa	Average value	$\frac{\sigma_{oct}}{\sigma_c}$	$\frac{\tau_{oct}}{\sigma_c}$	$\theta / ^\circ$
0.925	0.000	0.000		0.043	0.061	0
0.981	0.000	0.000	0.952	0.046	0.065	0
0.950	0.000	0.000		0.044	0.063	0
0.739	-0.5	-0.5		-0.012	0.082	0
0.808	-0.5	-0.5	0.754	-0.009	0.086	0
0.716	-0.5	-0.5		-0.013	0.080	0
0.602	-1.000	-1.000		-0.065	0.106	0
0.608	-1.000	-1.000	0.615	-0.065	0.106	0
0.635	-1.000	-1.000		-0.064	0.108	0

0.568	-1.500	-1.500		-0.114	0.137	0
0.575	-1.500	-1.500	0.589	-0.113	0.137	0
0.624	-1.500	-1.500		-0.111	0.140	0
0.315	-2.000	-2.000		-0.172	0.153	0
0.387	-2.000	-2.000	0.391	-0.169	0.158	0
0.471	-2.000	-2.000		-0.165	0.163	0
0.062	-2.500	-2.500		-0.231	0.169	0
0.128	-2.500	-2.500	0.112	-0.228	0.174	0
0.147	-2.500	-2.500		-0.227	0.175	0
-0.091	-3.000	-3.000		-0.285	0.192	0
-0.196	-3.000	-3.000	-0.172	-0.289	0.185	0
-0.230	-3.000	-3.000		-0.291	0.183	0
-0.787	-4.000	-4.000		-0.411	0.212	0
-0.716	-4.000	-4.000	-0.726	-0.407	0.217	0
-0.675	-4.000	-4.000		-0.405	0.220	0
-1.351	-5.000	-5.000		-0.530	0.241	0
-1.435	-5.000	-5.000	-1.362	-0.534	0.236	0
-1.300	-5.000	-5.000		-0.528	0.244	0

1

2

C: Results of plane tensile and compressive/axial tensile tests

σ_1/MPa	σ_2/MPa	σ_3/MPa	Average value	$\frac{\sigma_{oct}}{\sigma_c}$	$\frac{\tau_{oct}}{\sigma_c}$	$\theta / ^\circ$
0.947	0.108	-0.100		0.045	0.063	10.8
0.908	0.108	-0.100	0.945	0.043	0.061	11.3
0.980	0.108	-0.100		0.046	0.066	10.5
0.912	0.163	-0.150		0.043	0.062	16.7
0.925	0.163	-0.150	0.931	0.044	0.063	16.4
0.955	0.163	-0.150		0.045	0.065	15.9
0.885	0.271	-0.250		0.042	0.065	27.3
0.943	0.271	-0.250	0.902	0.045	0.068	25.8
0.879	0.271	-0.250		0.042	0.065	27.5
0.916	0.314	-0.290		0.044	0.069	30.1
0.887	0.314	-0.290	0.884	0.043	0.067	30.9
0.849	0.314	-0.290		0.041	0.065	32.0

0.780	0.379	-0.350		0.038	0.066	39.5
0.851	0.379	-0.350	0.850	0.041	0.069	37.0
0.918	0.379	-0.350		0.044	0.073	34.9
0.868	0.433	-0.400		0.042	0.074	40.3
0.893	0.433	-0.400	0.846	0.043	0.075	39.5
0.776	0.433	-0.400		0.038	0.069	43.5
0.834	0.509	-0.470		0.041	0.078	46.1
0.820	0.509	-0.470	0.819	0.040	0.077	46.6
0.802	0.509	-0.470		0.039	0.076	47.3
0.777	0.542	-0.500		0.038	0.078	50.0
0.659	0.542	-0.500	0.771	0.033	0.073	54.7
0.876	0.542	-0.500		0.043	0.082	46.5
0.695	0.650	-0.600		0.035	0.084	58.2
0.672	0.650	-0.600	0.746	0.034	0.083	59.1
0.871	0.650	-0.600		0.043	0.091	52.0
0.721	0.704	-0.65		0.036	0.090	59.4
0.687	0.704	-0.65	0.704	0.035	0.089	60.6
0.703	0.704	-0.65		0.035	0.089	60.0

1

2 **References:**

3 [1]J. Murali Krishnan, K.R. Rajagopal,Triaxial testing and stress relaxation of asphalt
4 concrete, J. Mechanics of Materials. 36 (2004) 849–864.

5 [2]Y.J. Qiao, X.R. Ma,Analysis on Shear Stress Design Index of Long-Life Asphalt
6 Pavement under Complex Traffic Conditions, J. Applied Mechanics and Materials.
7 743(2015)115-120.

8 [3] Yu Min Su, Nabil Hossiney, Mang Tia,Indirect Tensile Strength of Concrete
9 Containing Reclaimed Asphalt Pavement Using the Superpave Indirect Tensile
10 Test,J.Advanced Materials Research.723(2013)368-375.

11 [4]Sun Woo Park, Y. Richard Kim, Richard A. Schapery, A viscoelastic continuum
12 damage model and its application to uniaxial behavior of asphalt concrete,
13 J.Mechanics of Materials. 24(1996) 241-255.

- 1 [5] K. Mollenhauer, M. Wistuba, Evaluation of hot-mix asphalt susceptibility to
2 temperature-induced top-down fatigue cracking by means of Uniaxial Cyclic Tensile
3 Stress Test, *J. Road Materials and Pavement Design*.13(1)(2012)171-190.
- 4 [6] Lee Leon, Raymond Charles, Nicola Simpson, Stress-strain behaviour of asphalt
5 concrete in compression, *J. Procedia Structural Integrity*. 2(2016)2913-2920.
- 6 [7]Junyan Yi, ShihuiShen, BalasingamMuhunthan, DechengFeng, Viscoelastic–plastic
7 damage model for porous asphalt mixtures:Application to uniaxial compression and
8 freeze–thaw damage, *J.Mechanics of Materials*. 70(2014) 67–75.
- 9 [8]Quantao Liu, Erik Schlangen, Martin van de Ven, Gerbert van Bochove, Jo van
10 Montfort, Evaluation of the induction healing effect of porous asphalt concrete
11 through four point bending fatigue test, *J.Construction and Building Materials*.
12 29(2012) 403-409.
- 13 [9] Marco Pasetto, Nicola Baldo, Dissipated energy analysis of four-point bending test
14 on asphalt concretes made with steel slag and RAP, *J. International Journal of
15 Pavement Research and Technology*. 10(5)(2017)446-453.
- 16 [10] GuoweiZeng, XinhuaYang, Long Chen, Fan Bai, Damage Evolution and Crack
17 Propagation in Semicircular Bending Asphalt Mixture Specimens, *J.
18 ActaMechanicaSolidaSinica*. 29(6)(2016)596-609.
- 19 [11] GianlucaCerni, EdoardoBocci, FabrizioCardone, Alessandro Corradini,
20 Correlation Between Asphalt Mixture Stiffness Determined Through Static and
21 Dynamic Indirect Tensile Tests, *J. Arabian Journal for Science and Engineering*.
22 42(3)(2017)1295-1303.
- 23 [12]Dong Zhang, ShuguangHou, Jiang Bian, Liang He, Investigation of the
24 micro-cracking behavior of asphalt mixtures in the indirect tensile test, *J. Engineering
25 Fracture Mechanics*.163(2016) 416-425.
- 26 [13]S.A. Tan, B.H. Low, T.F. Fwa, Behavior of asphalt concrete mixtures in
27 triaxialcompression,*Journal of Testing and Evaluation*. 22 (5) (1994) 195–203.
- 28 [14]Yanqing Zhao, Jimin Tang, Hui Liu, Construction of triaxial dynamic modulus
29 master curve for asphalt mixtures,*J. Construction and Building
30 Materials*.37(2012)21–26.

- 1 [15]Jiantong Zhang, Jun Yang, Y. Richard Kim, Characterization of mechanical
2 behavior of asphalt mixtures under partial triaxial compression test,J.Construction and
3 Building Materials.79(2015)136–144.
- 4 [16] Lan Wang, Xiao HuiMeng, Li Qing Pan, JiQuan Zhang, The Triaxial Test
5 Research of Asphalt-Rubber Mixture,J.Advanced Materials
6 Research.598(2012)603-607.
- 7 [17] Bernhard Hofko, Ronald Blab, Enhancing triaxial cyclic compression testing of
8 hot mix asphalt by introducing cyclic confining pressure, J.Road Materials and
9 Pavement Design.15(1)(2014)16-34.
- 10 [18]Jingang Wang, André A.A. Molenaar, Martin F.C. van de Ven, Shaopeng Wu.
11 Behaviour of asphalt concrete mixtures under tri-axial compression, J.Construction
12 and Building Materials.105 (2016) 269–274
- 13 [19] Desai CS, Somasundaram S, Frantziskonis G. A hierarchical approach for
14 constitutive modelling of geologic materials, J.Numerical and Analytical Methods in
15 Geomechanics.10(3)(1986)225–57.
- 16 [20]Guan Hong-xin,Lilian-you,Yang Hui-you,Liuhao,LuoZeng-jie. Intermediate
17 Principal Stress Effect on Asphalt Mixture at low Temperature, J.China Journal of
18 Highway and Transport.27(11)(2014)11-16.45.
- 19 [21] Jenny Liu, Sheng Zhao, Lin Li, Peng Li, Steve Saboundjian. Low temperature
20 cracking analysis of asphalt binders and mixtures. J. Cold Regions Science and
21 Technology. 141 (2017) 78-85.
- 22 [22]TuoHuang.Study on triaxial test method and strength theory of asphalt mixture,
23 School of traffic and transportation engineering,Changsha University of Science &
24 Technology, Changsha, China. 2013
- 25 [23]JianlongZheng,TuoHuang.Study on triaxial test method and failure criterion of
26 asphalt mixture, J.Journal of traffic and transportation engineering (English edition).
27 2 (2) (2015) 93-106.
- 28 [24]Yupu Song,Constitutive relations and failure criterions of various concrete
29 materials. China Water Conservancy and Hydropower Press,2002

- 1 [25] Long Cheng, Vincent Monchiet, Léo Morin, Géry de Saxcé, Djimedo Kondo. An
- 2 analytical Lode angle dependent damage model for ductile porous materials. J.
- 3 Engineering Fracture Mechanics. 149 (2015) 119-133.